Simultaneous unwrapping and low pass filtering of continuous phase maps based on autoregressive phase model and wrapped Kalman filtering

Rishikesh Kulkarni[a], Pramod Rastogi[b]

[a] *Department of Electronics and Electrical Engineering, Indian Institute of Technology Guwahati, India*

[b] *Applied Computing and Mechanics laboratory, Ecole Polytechnique Fédérale de Lausanne, Switzerland*

Abstract

We propose a simultaneous noise filtering and phase unwrapping algorithm. Spatial evolution of phase is modeled as an autoregressive Gaussian Markov random field. Accordingly, phase value at a pixel is related to phase values at surrounding pixels in a probabilistic manner. The problem of estimation of these probabilities is formulated as state space analysis using the wrapped Kalman filter. Simulation and experimental results demonstrate the practical applicability of the proposed phase unwrapping algorithm.

Keywords: Phase unwrapping, Gaussian Markov random field, Autoregressive model, State Space Analysis, Wrapped Kalman Filter.

1. Introduction

Measurement techniques such as optical interferometry [1, 2], interferometric synthetic aperture radar [3], tomographic imaging [4], fringe projection profilometry [5] and magnetic resonance imaging [6] involve measurement of phase which is essentially proportional to the particular physical parameter of interest [7]. Typically, the measurement is obtained in the form of a complex interferogram which at a point (x, y) can be expressed as

$$I(x, y) = \exp\left[j\phi(x, y)\right] + \epsilon(x, y) \tag{1}$$

where, $I(x, y)$ is the complex interference field; $j = \sqrt{-1}$; $\phi(x, y)$ is the phase and $\epsilon(x, y)$ is the complex additive white Gaussian noise. Here, we have considered the commonly used additive noise model. The physical parameter of

interest can be quantified using an accurate estimate of the phase. However, only a modulo 2π value of the phase, termed as the *wrapped phase*, can be determined from the measurement of the form given in Eq. (1). The relationship between the wrapped phase and absolute phase can be expressed as

$$\psi(x, y) = \mathcal{W}\{\phi(x, y)\}, \tag{2}$$

where, $\mathcal{W}\{\cdot\}$ is an operator which wraps the values of absolute phase $\phi(x, y)$ in the range of $(-\pi, \pi]$. Since the physical parameter is proportional to the absolute phase, an inverse of phase wrapping operation, i.e., *phase unwrapping* (PU), becomes indispensable. The PU operation can be expressed as equivalent to finding appropriate integer multiples of 2π at each pixel as

$$\phi(x, y) = \psi(x, y) + 2\pi K(x, y), \tag{3}$$

where, $K(x, y)$ represents the two-dimensional integer field that needs to be computed. PU is a simple operation if the absolute phase is spatially continuous and measurement is noise-free. The unwrapped phase estimate can be obtained based on Itoh's method [8] wherein the absolute phase is evaluated at each pixel by equating the phase difference at consecutive pixels with the corresponding wrapped phase difference under the assumption that the absolute phase difference is no more than π. However, such an assumption is violated in the presence of noise and/or under-sampling in the phase measurement. Apart from these practical issues, difficulty in PU may be enhanced further due to the presence of inherent phase discontinuities in the absolute phase. Since these issues contribute to making PU very difficult, much research effort has been devoted to design robust unwrapping algorithms [9, 10].

Few examples of unwrapping methods are those based on branch-cut [11, 12, 13, 14], quality guided [15, 16, 17, 18], least-squares algorithms [20, 21, 22, 23], and polynomial phase approximation [24, 25]. Whereas some of these algorithms are inherently noise robust [26], some algorithms require phase denoising as an essential pre-processing operation [27, 28, 29]. Recently, a number of PU algorithms have been proposed based on the use of Kalman filtering [30, 31, 32, 33, 34, 35]. The proposed algorithm belongs to this category of unwrapping methods. The spatial phase variation is modelled as an autoregressive (AR) process. The AR coefficients estimation is formulated as a state estimation performed using the wrapped Kalman filter.

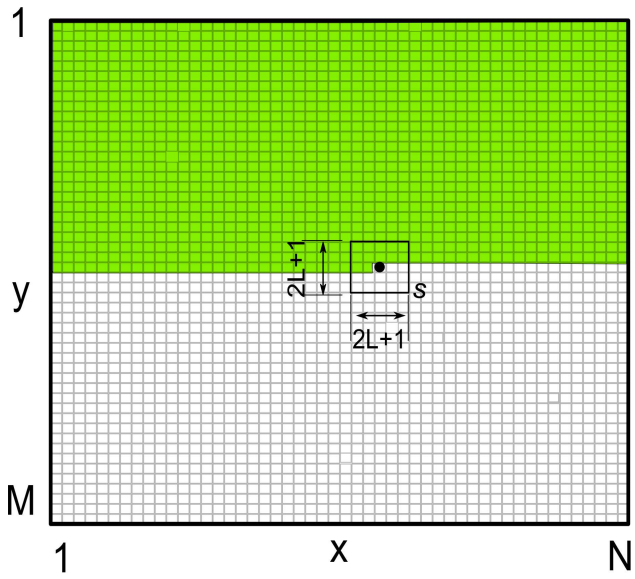

Figure 1: Horizontal, left to right, top to bottom scanning of the phase fringe pattern. The shaded and unshaded portions show the unwrapped and wrapped regions, respectively.

2. Proposed Method

2.1. Autoregressive Gaussian Markov Random Field Phase Model

In this paper, we consider an autoregressive Gaussian Markov random field (AR-GMRF) model of absolute phase distribution. Different PU algorithms based on Markov randow field model have been proposed in the literature [36, 37, 40, 41, 42]. However, most of these algorithms formulate an optimization problem for the estimation of an integer field $K(x, y)$.

Although the phase unwrapping approach proposed in this paper differs from these algorithms, in some sense it might still keep some similarities with the PU algorithms proposed in [37, 38, 39]. Nevertheless, as discussed in the text below the state space formulation considered in this paper does differ significantly from these algorithms. We model the absolute phase as a sample of causal nonsymmetrical half-plane AR-GMRF [37];

$$\phi(x, y) = \sum_{(x',y')\in\mathcal{S}} \alpha_{x,y}(x', y')\phi(x', y'). \tag{4}$$

Essentially, the absolute phase at (x, y) is evaluated based on its prior knowledge over the support $\mathcal{S}$ in a probabilistic manner. The support $\mathcal{S}$

is defined in Fig. 1 where the fringe pattern is scanned horizontally from left to right, top to bottom. The shaded portion in the figure indicates the already unwrapped area prior to the current pixel (x, y). We consider a square window around the current pixel, the latter being denoted as a dot. The support $\mathcal{S}$ basically includes the pixels which are processed prior to the current pixel. For example, with a window of size L we have $\{x', y'\}$: $(x' = x$ and $y - L \leq y' < y)$ or $(x - L \leq x' < x$ and $y - L \leq y' \leq y + L)$. The probabilities $\alpha_{x,y}(x', y')$ can be considered as the weights of neighboring phase values contributing to the phase value at the current pixel. The method proposed in [37, 38, 39] considers these weights to be known a priori. However, such an assumption in practice might be severely restrictive in achieving a reliable PU. On the other hand, α is sub-scripted with (x, y) to indicate that in the proposed algorithm the probabilities (weights) are spatially varying.

2.2. State Space Formulation

We propose a technique to evaluate weights $\alpha(x, y)$ at each pixel. In order to do so, we consider the first order difference equation model of the spatial evolution of weights as

$$\alpha_l(x', y') = \alpha_{l-1}(x', y') + \delta_l(x', y'), \tag{5}$$

where, subscripts l and $l-1$ represent the estimates obtained at the current and the immediate past pixel, respectively; $\delta_l(x', y')$ represents a random perturbation of weight vector modeled as the Gaussian white noise with zero mean and pre-defined variance μ^2. Based on Eqs. (4) and (5), a state space formulation is considered with a state vector $\boldsymbol{\alpha}$ defined as

$$\begin{aligned}\boldsymbol{\alpha} = [&\alpha(x - L, y - L), \alpha(x - L, y - L + 1), \cdots, \\ &\alpha(x, y - L), \cdots, \alpha(x, y - 1)]^T.\end{aligned} \tag{6}$$

where the subscript of α is not shown for notation simplicity. The size of state vector is $2L(L + 1) \times 1$. The process update of state vector is given as

$$\boldsymbol{\alpha}_l = \boldsymbol{F}\boldsymbol{\alpha}_{l-1} + \boldsymbol{G}\boldsymbol{\epsilon}_l \tag{7}$$

where $\boldsymbol{F}$ and $\boldsymbol{G}$ are identity matrices of size $2L(L+1) \times 2L(L+1)$. The most common observation model considered in analyzing complex interference field is given as below:

$$\boldsymbol{\psi}_l = \begin{bmatrix}\cos\phi(x, y) \\ \sin\phi(x, y)\end{bmatrix} + \begin{bmatrix}\epsilon_c(x, y) \\ \epsilon_s(x, y)\end{bmatrix}, \tag{8}$$

where, ϵ_c and ϵ_s indicate the real and imaginary parts of ϵ, respectively. Since the observation vector is a nonlinear function of phase, a nonlinear recursive filter such as the extended Kalman filter (EKF) or unscented Kalman filter (UKF) are used. Recently, a *wrapped Kalman filter* has been proposed as an alternative to EKF and UKF for recursive Bayesian inference of circular variable [43]. As mentioned in [43], since we have a 1D measurement of $\psi(x, y)$, the 2D observation model in Eq. (8) introduces additional noise to the system. Accordingly, we consider the wrapped phase observation model as

$$\begin{aligned} \psi_l &= \psi(x, y) + \eta_l \\ &= \mathcal{W}\left\{\boldsymbol{H}_l \boldsymbol{\alpha}_l\right\} + \eta_l \end{aligned} \tag{9}$$

where,

$$\begin{aligned} \boldsymbol{H}_l = [&\phi(x - L, y - L), \phi(x - L, y - L + 1), \cdots, \\ &\phi(x, y - L), \cdots, \phi(x, y - 1)], \end{aligned} \tag{10}$$

and η_l represents noise associated with the wrapped phase measurement. It has been shown that the performance of the WKF is better compared to the EKF and UKF in the circular variable state estimation. We propose to utilize the WKF with state space model represented by Eqs. (7) and (9).

2.3. The Wrapped Kalman Filter Implementation

Before moving on to the discussion on the WKF implementation, an important point to note here is that the term $\boldsymbol{H}_l \boldsymbol{\alpha}_l$ essentially represents the absolute phase $\phi(x, y)$. Since the absolute phase itself can be modeled as a random variable with normal distribution, say $\phi = \mathcal{N}(\phi_m, \sigma_\phi^2)$, the wrapped Gaussian distribution of associated measurement ψ is obtained as [44],

$$P(\psi; \phi_m, \sigma_\phi^2) = \sum_{k=-\infty}^{\infty} \frac{1}{\sqrt{2\pi\sigma_\phi^2}} \exp\left[-\frac{(\psi - (\phi_m + 2\pi k))}{2\sigma_\phi^2}\right]. \tag{11}$$

The above described circular statistics is used in the WKF implementation to compute the a posteriori state estimate. The procedure of state estimation based on the WKF is given as follows [43, 45, 46, 47]:

1. Initialize the state vector estimate at $l = 0$ and its error covariance matrix as

$$\hat{\boldsymbol{\alpha}}_0^+ = \mathbb{E}\left[\boldsymbol{\alpha}_0\right], \tag{12}$$

$$\boldsymbol{P}_0^+ = \mathbb{E}\left[\left(\boldsymbol{\alpha}_0 - \hat{\boldsymbol{\alpha}}_0^+\right)\left(\boldsymbol{\alpha}_0 - \hat{\boldsymbol{\alpha}}_0^+\right)^T\right], \tag{13}$$

where, $\mathbb{E}$ is the expectation operator. The superscripts $-$ and $+$ indicate the *a priori* and *a posteriori* estimates of the associated variables.

2. The process updates of the state vector and error covariance at the lth step are computed as

$$\hat{\boldsymbol{\alpha}}_l^- = \boldsymbol{F}\hat{\boldsymbol{\alpha}}_{l-1}^+, \tag{14}$$

$$\boldsymbol{P}_l^- = \boldsymbol{F}\boldsymbol{P}_{l-1}^+\boldsymbol{F}^T + \boldsymbol{G}\boldsymbol{\Xi}\boldsymbol{G}^T. \tag{15}$$

where, $\boldsymbol{\Xi}$ is a diagonal matrix with μ^2 along its diagonal.

3. The unwrapped phase estimate at (x, y) is computed using the predicted state vector as

$$\hat{\phi}_l = \boldsymbol{H}_l\hat{\boldsymbol{\alpha}}_l^-. \tag{16}$$

4. The observation update of the state vector and its error covariance matrix is performed based on the Kalman gain as

$$\boldsymbol{K}_l = \boldsymbol{P}_l^-\boldsymbol{H}_l^T\left(\boldsymbol{H}_l\boldsymbol{P}_l^-\boldsymbol{H}_l^T + \Sigma\right)^{-1}, \tag{17}$$

$$\hat{\boldsymbol{\alpha}}_l^+ = \hat{\boldsymbol{\alpha}}_l^- + \boldsymbol{K}_l\mathcal{W}\left(\psi_l - \hat{\phi}_l\right), \tag{18}$$

$$\boldsymbol{P}_l^+ = \left(\boldsymbol{I} - \boldsymbol{K}_l\boldsymbol{H}_l\right)\boldsymbol{P}_l^-\left(\boldsymbol{I} - \boldsymbol{K}_l\boldsymbol{H}_l\right)^T + \boldsymbol{K}_l\Sigma\boldsymbol{K}_l^T, \tag{19}$$

where, $\boldsymbol{K}_l$ is the Kalman gain; $\boldsymbol{I}$ is an identity matrix of size $2L(L+1) \times 2L(L+1)$ and Σ is the pre-defined measurement error covariance. Equation (18) indicates that the difference between the estimated unwrapped phase and measured wrapped phase is *wrapped* prior to the observation update of the state vector. This step differs from the observation state update considered in the design of wrapped Kalman filter [43]. As the main objective of the algorithm proposed in [43] is to accurately estimate the circular(wrapped) variable from noisy observations, it is required that the prior state estimate ($\hat{\boldsymbol{\alpha}}_l^-$) is wrapped before the observation update. On the other hand, such wrapping of the observation estimate is not required in the proposed method since the state

vector does not contain a circular variable element [35]. Considering the wrapped Gaussian statistics given in (10), the innovation term is derived from multiple replicas of the observation [43]. However, it has been shown that three such replicas are sufficient in obtaining accurate state estimate. In the practical implementation of our algorithm, we have observed that the measurement replicas do not have significant effect on the performance of PU. We have, therefore, implemented the algorithm considering the observation without replicas.

5. The steps from 1 to 4 are implemented at each pixel location to obtain the two dimensional unwrapped phase estimate.

It is evident that past phase information is not available at few initial pixels. Accordingly, the vector H_l is initialized with a pre-defined constant value of phase ϕ_{init}. This vector is updated as and when the estimated phases associated with the pixels surrounding the pixel being operated are available. To improve the robustness of the PU algorithm, the state vector and its error covariance matrix are initialized as an average of their estimated values evaluated at neighboring pixels. According to Eq. (10), $\kappa = 2L(L+1)$ past phase values are used to predict the phase value at the current pixel. Since we have considered the AR model of the spatial phase evolution, κ essentially defines the AR model order. If a high window size L is considered, the AR model order is sufficiently high. However, in practice, the phase estimate can be computed with much lower AR model order.

Depending on the measurement setup or the observed physical parameter, the region(s) of the fringe map may need to be masked to bypass the invalid regions. Such situations may arise due to the improper object illumination or signal decorrelation. In such cases, the past phase data selection described in Fig. 2 has to be modified. The vector $\boldsymbol{H}_l$ may not contain κ number of estimated unwrapped phase values. It is therefore appended with constant phase values such that the state vector length is κ. Another approach is by adaptive selection of the neighbor pixel values to build the $\boldsymbol{H}_l$ vector.

The WKF implementation requires the initialization of certain variables. For example, $\hat{\boldsymbol{\alpha}}_0^+ = \frac{1}{\kappa}[1, 1, \cdots, 1]$, $\hat{\boldsymbol{P}}_0^+ = 10^3 \cdot \boldsymbol{I}$ and $\Sigma = 10^3$. Although, these values are selected empirically as is usually done in any Kalman filtering applications, the proposed method is not highly sensitive to their variations. Since the noise strength in an experimentally recorded wrapped phase map cannot be known apriori, we always set a high value of noise covariance considering an overestimate of the noise strength. Consequently, the proposed

SNR(in dB)	κ (no. of past samples used)					PhaseLa	LSPU	Goldstein
	4	6	8	10	12			
0	0.9	0.08	**0.08**	0.09	0.1	9.13	7.15	3.82
1	0.08	0.04	0.04	0.04	**0.04**	6.27	3.21	0.9
2	0.07	0.04	0.03	0.03	0.03	**0.02**	1.92	0.62

Table 1: Mean square errors (in radians) in the unwrapped phase estimation for the phase example given in Fig. 2a.

method is capable of unwrapping wrapped phase maps with a wide range noise strengths. However, an apriori knowledge of noise strength certainly helps in appropriate selection of value Σ. The covariance matrix $\boldsymbol{\Xi}$ is set depending on the magnitude of phase variations. A large value is set for fast varying phase in order to update the state vector at the same rate. Likewise, a low value is set for slowly varying phase.

3. Simulation and Experimental Results

The proposed method is validated with simulation and experimental examples. In the first example, a phase fringe pattern generated with signal to noise ratio (SNR) of 0 dB is shown in Fig. 2a. The SNR is defined according to the fringe model given in Eq. (8). The unwrapped phase shown in Fig. 2b is computed using $\kappa = 4$ and $\boldsymbol{\Xi} = 10^{-5} \cdot \boldsymbol{I}$. Figure 2c shows the histogram of unwrapped phase error. It can be observed that the proposed method performed accurate phase unwrapping displaying expected zero-mean Gaussian error distribution. Further, we consider a realistic simulation of the speckle noise corrupted phase pattern as described in [48]. Accordingly, in practice, the high density fringe areas are more severely corrupted by the speckle noise compared to the low density areas. This aspect is cannot be included in the measurement model given in Eq. (8). The speckle noise corrupted phase fringe pattern simulated in Fig. 2d contains high fringe density areas marked by circles which are highly corrupted by the speckle noise in comparison to low fringe density areas. For this example , the proposed algorithm was found to provide accurate unwrapped phase estimate as shown in Fig. 2e. The histograms of phase unwrapping error shown in Fig. 2f exhibits the expected second-order probability distribution of error. The performance of the proposed method is evaluated against three representative PU algo-

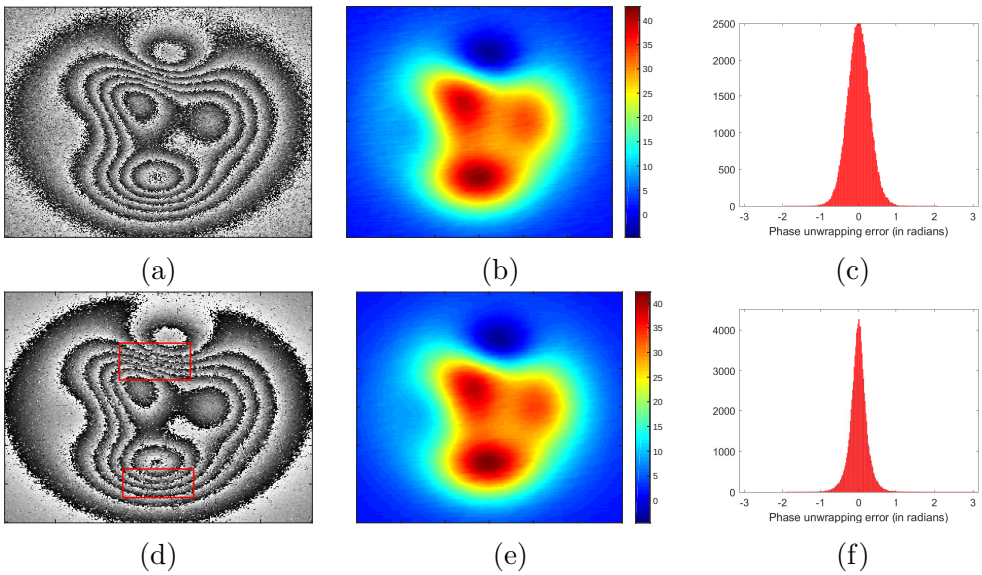

Figure 2: (a) Phase fringe pattern simulated at SNR = 0 dB; (b) unwrapped phase estimate obtained with $\kappa = 4$; (c) histogram of unwrapped phase error; (d) speckle noise corrupted phase fringe pattern; (e) unwrapped phase estimate with $\kappa = 4$ and (f) histogram of unwrapped phase error. All phase values are in radians.

rithms: least squares phase unwrapping (LSPU) algorithm [19], model based PU algorithm based on local polynomial phase approximation (PhaseLA) [24] and Goldstien's branch-cut PU algorithm. Simulations were performed at 0, 1, 2 dB SNRs. The phase unwrapping error results are tabulated in tables 1 and 2. Whereas, table 1 shows the mean square error, table 2 shows the peak-to-valley error in the unwrapped phases. The proposed algorithm was found to perform better compared to the rest of the algorithms. Especially, it can be observed that the use of a higher number of past phase values (κ) in the proposed algorithm provides improved PU accuracy. At SNR = 2 dB, the PhaseLA method provided lower mean square error compared to the proposed method. However, for the same case, the peak-to-valley error was found to be significantly higher for the PhaseLA method compared to the proposed method.

One of the important features of the proposed algorithm is demonstrated with the second simulation example given in Fig. 3. Most of the PU algorithms are based on the assumption that the maximum phase difference between two consecutive pixels is less that π. This assumption becomes in-

SNR(in dB)	κ (no. of past samples used)					PhaseLa	LSPU	Goldstein
	4	6	8	10	12			
0	3.5	3.65	**3.38**	3.5	4.5	19.57	16.96	53.75
1	2.77	2.32	2.04	1.98	**1.89**	19.12	12.63	51.68
2	2.24	1.93	1.93	**1.88**	1.94	7.38	10.79	41.95

Table 2: Peak-to-valley errors (in radians) in the unwrapped phase estimation for the phase example given in Fig. 2a.

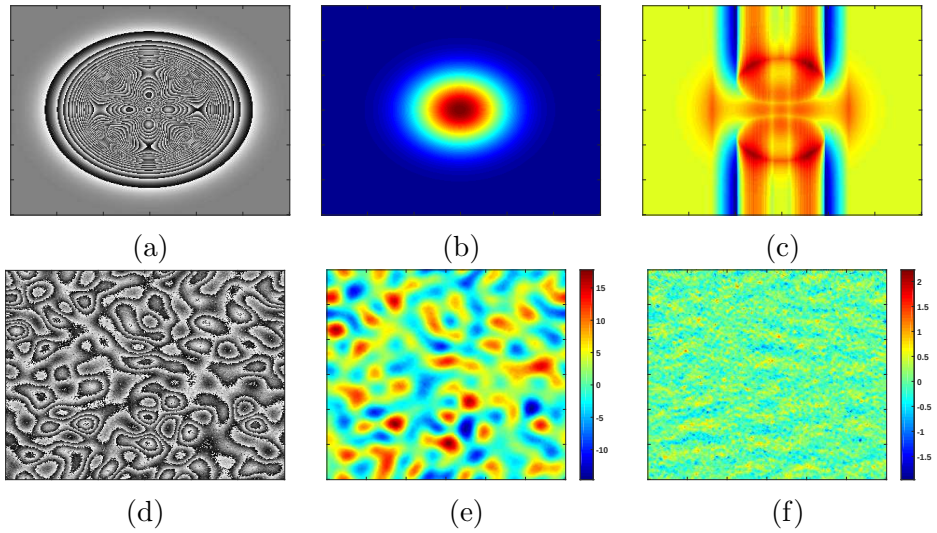

Figure 3: (a) Undersampled phase fringe pattern; (b) unwrapped phase; (c) unwrapped phase calculated using Itoh's method. (d) phase fringe pattern with random spatial variation; (e) unwrapped phase and (f) error in the estimated unwrapped phase. All phase values are in radians.

valid if aliasing occurs with the under-sampled phase measurement [49, 50]. The AR-GMRF phase model is shown to be capable of capturing phase evolution even in the presence of phase under-sampling [37]. Figure 3a shows one such example of noiseless phase map. The unwrapped phase estimate in Fig. 3b clearly indicates the reliability of the proposed algorithm even in the case of aliased phase measurement. On the other hand, the Itoh's method failed to provide accurate unwrapped phase estimate as shown in Fig. 3c even in the absence of noise. Another example of a fringe pattern with smooth yet random phase distribution is shown in Fig. 3d. Since the

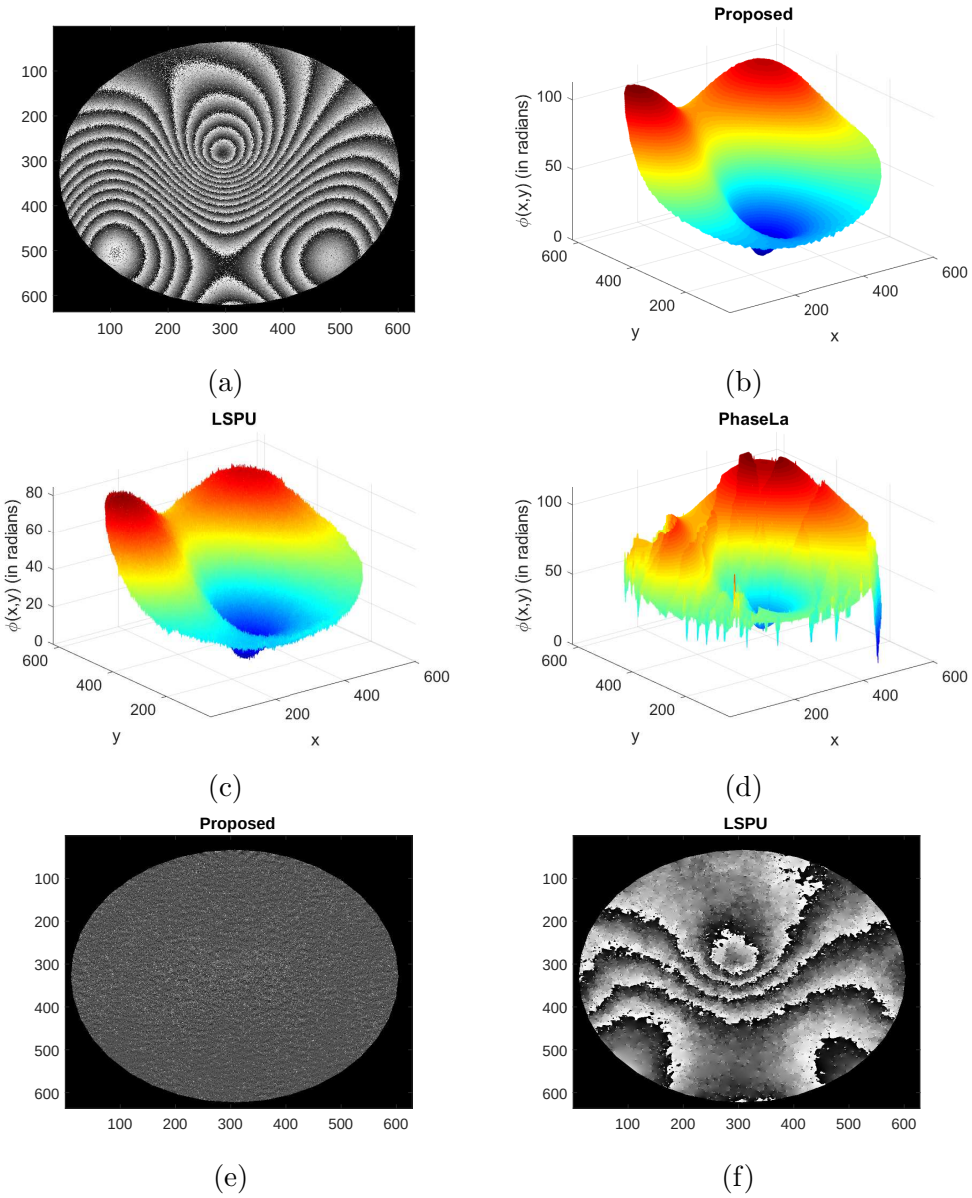

Figure 4: (a) Fringe pattern corresponding to out-of-plane deformation of an aluminum plate recorded in a digital holographic interferometry setup; unwrapped phase computed using (b) proposed method with $\kappa = 8$; (c) the LSPU algorithm and (d) the PhaseLa method. Residual phase corresponding to (e) the proposed method and (f) the LSPU method. All phase values are in radians.

proposed algorithm is capable of tracking random variations in the phase map by allowing random perturbations in the state vector elements, an accurate estimate of unwrapped phase is obtained in Fig. 3e. Figure 3f shows the phase unwrapping error map.

For the experimental validation of the proposed method, we considered the phase fringe pattern in Figure 4a. This fringe pattern is associated with an out-of-plane deformation of a square aluminum plate recorded in a digital holographic interferometry setup. Note that the phase information is available only on the illuminated surface. Accordingly, the light illuminated area is selected manually to create a binary mask. As mentioned earlier, the pixels with past phase information have to be selected by bypassing the masked pixels during the formation of $\boldsymbol{H}_l$ vector. By doing so, unwrapped phase estimate is obtained in the valid fringe region with $\kappa = 8$ as shown in Fig. 4b. Figures 4c and 4d show the unwrapped phase estimates obtained using the least-squares and the PhaseLA methods, respectively. The phaseLA method was found to provide unreliable phase estimate. The comparison of the unwrapping accuracy between the proposed method and least-squares method is provided with the residual phase maps shown in Figs. 4e and 4f, respectively. The comparison shows the improved unwrapping accuracy provided by the proposed method over the least-squares method.

4. Conclusion

A novel PU algorithm based on the AR-GMRF phase model is proposed which is capable of providing unwrapped phase estimate of the wrapped phase pattern consisting of random spatial variations. The WKF based state estimation offers noise robustness to the PU operation. The simulation and experimental results demonstrate the practical applicability of the proposed method.

References

[1] Xia H, Montresor S, Guo R, Li J, Olchewsky F, Desse J, and Picart P. Robust processing of phase dislocations based on combined unwrapping and inpainting approaches. Opt Lett 2017;42:322–325.

[2] Wu S, Zhu L, Pan S, Yang L. Spatiotemporal three-dimensional phase unwrapping in digital speckle pattern interferometry. Opt Lett 2016;41:1050–1053.

[3] Osmanoglu B, Sunar F, Wdowinski S, Cabral-Cano E.Time series analysis of insar data: Methods and trends. ISPRS J Photogrammetry and Rem Sens 2016;115:90–102.

[4] Grzegorczyk T M, Meaney P M, Jeon S I, Geimer S D, Paulsen K D. Importance of phase unwrapping for the reconstruction of microwave tomographic images. Biomed Opt Exp 2011;2:315-330.

[5] Su X, Zhang Q. Dynamic 3-d shape measurement method: A review. Opt Lasers Eng 2010;48:191–204.

[6] Jenkinson M. Fast, automated, n-dimensional phase-unwrapping algorithm. Mag Res Med 2003;49:193–197.

[7] Kulkarni R and Rastogi P.*Single and Multicomponent Digital Optical Signal Analysis* (IOP publishing, 2017).

[8] K. Itoh. Analysis of the phase unwrapping algorithm. Appl Opt 1982;21:2470-2470.

[9] Ghiglia D C, Pritt M D. *Two-dimensional phase unwrapping : theory, algorithms, and software* (J. Wiley & Sons, New York, 1998).

[10] Zappa E, Busca G. Comparison of eight unwrapping algorithms applied to fourier-transform profilometry. Opt Lasers Eng 2008;46:106–116.

[11] Cusack R, Huntley J M, Goldrein H T. Improved noise-immune phase-unwrapping algorithm. App Opt 1995;34:781–789.

[12] Zheng D and Da F. A novel algorithm for branch cut phase unwrapping. Opt Lasers Eng 2011;49:609–617.

[13] Karout S A, Gdeisat M A, Burton D R, Lalor M J. Two-dimensional phase unwrapping using a hybrid genetic algorithm. App Opt 2007;46:730–743.

[14] De Souza J C, Oliveira M E, Dos Santos P M. Branch-cut algorithm for optical phase unwrapping. Opt Lett 2015;40:3456–3459.

[15] Zhao M, Huang L, Zhang Q, Su X, Asundi A, Kemao Q. Quality-guided phase unwrapping technique: Comparison of quality maps and guiding strategies. App Opt 2011; 50:6214–6224.

[16] Su X and Chen W. Reliability-guided phase unwrapping algorithm: A review. Opt Lasers Eng 2004;42,245–261.

[17] Zhang S, Li X, Yau S. Multilevel quality-guided phase unwrapping algorithm for real-time three-dimensional shape reconstruction. App Opt 2007;46:50–57.

[18] Kemao Q, Gao W, Wang H. Windowed fourier-filtered and quality-guided phase-unwrapping algorithm. App Opt 2008;47,5420–5428.

[19] Ghiglia D C, Romero L A. Robust two-dimensional weighted and unweighted phase unwrapping that uses fast transforms and iterative methods. J Opt Soc Am A 1994;11:107–117.

[20] Ghiglia D C, Romero L A. Minimum lp-norm two-dimensional phase unwrapping. J Opt Soc Am A 1996;13:1999–2013.

[21] Wang X, Fang S, Zhu X. Weighted least-squares phase unwrapping algorithm based on a non-interfering image of an object. App Opt 2017;56:4543–4550.

[22] Zhao Z, Zhao H, Zhang L, Gao F, Qin Y, Du H. 2d phase unwrapping algorithm for interferometric applications based on derivative zernike polynomial fitting technique. Meas Sci Tech 2017;26:017001.

[23] Guo Y, Chen X, Zhang T. Robust phase unwrapping algorithm based on least squares. Opt Lasers Eng 2014;63:25–29.

[24] Katkovnik V, Astola J, Egiazarian K. Phase local approximation (phasela) technique for phase unwrap from noisy data. IEEE Tran Img Proc 2008;17:833–846.

[25] Gorthi S S, Rastogi P. Piecewise polynomial phase approximation approach for the analysis of reconstructed interference fields in digital holographic interferometry. J Opt 2009;11:065405.

[26] Servin M, Marroquin J L, Malacara D, Cuevas F J. Phase unwrapping with a regularized phase-tracking system. App Opt 1998;37:1917-1923.

[27] Aebischer H A, Waldner S. Simple and effective method for filtering speckle-interferometric phase fringe patterns. Opt Comm 1999;162:205–210.

[28] Kemao Q.Two-dimensional windowed Fourier transform for fringe pattern analysis: Principles, applications and implementations. Opt Lasers Eng 2007;45:304–317.

[29] Kemao Q, Nam L T H, Feng L, Soon S H. Comparative analysis on some filters for wrapped phase maps. App Opt 2007;46:7412–7418.

[30] Loffeld O, Nies H, Knedlik S, Yu W. Phase unwrapping for sar interferometry - a data fusion approach by Kalman filtering. IEEE Tran. on Geosci and Rem Sen 2008;46:47–58.

[31] Gurov I, Volynsky M. Interference fringe analysis based on recurrence computational algorithms. Opt Lasers Eng 2012;50:514–521.

[32] Waghmare R G, Mishra D, Subrahmanyam GRKS, Banoth E, Gorthi S S. Signal tracking approach for phase estimation in digital holographic interferometry. App Opt 2014;53:4150–4157.

[33] Xie X M, Li Y H. Enhanced phase unwrapping algorithm based on unscented Kalman filter, enhanced phase gradient estimator, and path-following strategy. App Opt 2014;53:4049–4060.

[34] Cheng Z, Liu D, Yang Y, Ling T, Chen X, Zhang L, Bai J, Shen Y, Miao L, Huang W.Practical phase unwrapping of interferometric fringes based on unscented Kalman filter technique. Opt Exp 2015;23:32337–32349.

[35] Kulkarni R, Rastogi P. Phase unwrapping algorithm using polynomial phase approximation and linear Kalman filter. App Opt 2018;57:702-708.

[36] Marroquin J L, Tapia M, Rodriguez-Vera R, Servin M. Parallel algorithms for phase unwrapping based on markov random field models. JOSA A 1995;12:2578-2585.

[37] Leitao JMN, Figueiredo MAT. Absolute phase image reconstruction: a stochastic nonlinear filtering approach. IEEE Tran Img Proc 1998;7:868-882.

[38] Estrada J C, Servin M, Quiroga J A. Noise robust linear dynamic system for phase unwrapping and smoothing. Opt Exp 2011;19:5126-5133.

[39] Navarro M A, Estrada J C, Servin M, Quiroga J A, Vargas J. Fast two-dimensional simultaneous phase unwrapping and low-pass filtering. Opt Exp 2012;20:2556-2561.

[40] Bioucas-Dias J M, Leitäo JMN. The ZπM algorithm: A method for interferometric image reconstruction in SAR/SAS. IEEE Tran Img Proc 2002;11:408-422.

[41] Ying L, Liang Z, Munson D C, Koetter R, Frey B J. Unwrapping of MR phase images using a Markov random field model. IEEE Tran Med Img 2006;25:128-136.

[42] Bioucas-Dias J M, Valadão G. Phase unwrapping via graph cut. IEEE Tran Img Proc 2007;16:698-709.

[43] Traa J, Smaragdis P. A wrapped Kalman filter for azimuthal speaker tracking. IEEE Sig Proc Lett 2013;20:1257-1260.

[44] Mardia K V, Jupp P E. *Directional Statistics* (John Wiley & Sons, Inc., 2008).

[45] Kalman R E. New Approach to Linear Filtering and Prediction Problems. J Fluids Engg, Trans ASME 1960;82:35-45.

[46] Simon D. *Optimal State Estimation: Kalman, H Infinity, and Nonlinear Approaches* (Wiley-Interscience, 2006).

[47] Grewal M S, Andrews A P. *Kalman Filtering: Theory and Practice Using MATLAB* (Second Edition, John Wiley & Sons, Inc., 2015).

[48] Montresor S, Picart P. Quantitative appraisal for noise reduction in digital holographic phase imaging. Opt Exp 2016;24:14322-14343.

[49] Greivenkamp J E. Sub-Nyquist interferometry. App Opt 1987;26:5245-5258.

[50] Servin M, Malacara D, Cuevas F J. Path-independent phase unwrapping of subsampled phase maps. App Opt 1998;35:1643:1649.